

A Novel Load Adaptive ZVS Auxiliary Circuit For PWM Three-Level DC–DC Converters

**Arugonda Vandana****M.Tech****Arjun College of Technology and Sciences.****S.Vijay, M.Tech****Power Electronics, Assistant Professor,****Arjun College of Technology and Sciences.**

Abstract:

Three-level PWM dc–dc converters convert high dc voltage (>500 V) generally at the output of a three-phase ac–dc PWM rectifier in ac–dc converters to an isolated dc output voltage which can be used to power data center loads. Strict efficiency requirements at loads from 20% to 50% of full load of ac–dc converters for telecom applications have been introduced by energy star enforcing industries to improve efficiency of the dc–dc converter in an ac–dc converter powering data-center loads at those loads. High-efficiency requirements at low and mid loads in high switching frequency PWM dc–dc three-level converters implemented with MOSFETs can be achieved by reducing switching losses through optimized load adaptive ZVS for the entire load range. In this paper, a simple yet novel load adaptive ZVS auxiliary circuit for three-level converter is proposed for so that the resulting three-phase ac–dc converter can meet energy star platinum efficiency standard.

INTRODUCTION:

Three-level dc–dc converters are used for dc–dc conversion with galvanic isolation when the input voltage is typically higher than 500 V dc. Fig. 1 shows a three level dc–dc converter. The key advantage of this topology compared to the conventional dc–dc full-bridge converter in high voltage applications is that the input dc voltage is split equally so that the peak voltage stress of the semiconductor devices and the dc bus capacitors are reduced to half of the input dc voltage.

Although there exists quite a few three-phase ac-to-dc rectifiers with input power factor correction (PFC) [11], the PWM three-phase boost-type rectifier shown in Fig. 2(a) is one of the simplest and cheapest three-phase active rectifier which is often used in industrial converters for three-phase ac-to-dc power conversion with input PFC. In order to reduce overall energy consumption by data centers and telecom loads, U.S. Environmental Protection Agency (EPA), Energy Star and Climate Savers Computing initiative documents, [27]–[30] have set up strict efficiency requirements for converters used in telecom and IT systems and other plug loads powered by the utility mains. According to such regulatory agencies ac–dc converters for plug load applications should have high-efficiency values at loads ranging from 20% to 50% of full load to fulfill the strict requirements of Energy Star “Platinum Efficiency Standards.”

The corresponding efficiency curve of an ac–dc converter meeting Platinum Efficiency standard is shown in Fig. 2(b). It should also be noted that presently lightload and mid-load efficiencies of such ac–dc converters are of utmost importance compared to the full load efficiency since such converters always operate in parallel with similar converters along with load cycling so that during their operating cycle these converters mostly operate from 20% to 60% of full load. It is this typical load profile of most frequent operation of the converter that has enforced agency standards like Energy Star to develop such strict efficiency requirements at low and mid loads of a converter.

Full range soft switching from no load to full load is also important for reducing overall EMI of the converter leading to size and weight reduction of the EMI filter components which constitute to the converter weight and volume. Three-level dc–dc converters can be classified into following categories according to the soft switching techniques that they use.

Exciting concept:

- A. ZCS and ZCZVS PWM Three-Level DC–DC Converter
- B. Resonant Three-Level DC–DC Converter.
- C. Conventional PWM Three-Level DC–DC Converter With Natural ZVS
- D. ZVS PWM DC–DC Three-Level Converters With Entire Load Range ZVS Capability

Proposed concept:

Proposed ZVS PWM DC–DC Three-Level Converters With Load Adaptive ZVS.

In order to overcome the issues associated with load adaptive ZVS in three-level PWM dc–dc converters, a new three-level converter topology is proposed in this paper, as shown in Fig. 3. A simple load adaptive ZVS auxiliary circuit consisting of auxiliary inductors La1 and La2 , dc bus-splitting capacitors Cb1 , Cb2 , and flying capacitors Cb3 and Cb4 , which are also involved in the voltage balancing mechanism along with clamping diodes Dc1 and Dc2 is shown in Fig. 3. A dc blocking capacitor Cblk is necessary to block any dc voltage in the transformer primary winding. The auxiliary windings La1 and La2 are magnetically coupled with an effective turns ratio of 1:1 and inductance of LC are the key components of the auxiliary circuit.

Operation principle:

To emphasize the importance of the proposed converter for meeting Energy Star Platinum efficiency standards discussed earlier, experimental efficiency results of the proposed converter cascaded with a

front-end three phase PWM ac–dc rectifier, those of the converter in [2] when cascaded with the same ac–dc three-phase converter are presented and compared. 4) Section V presents a comparative study of proposed converter with the conventional PWM three-level dc–dc converter and other extended range three-level PWM converters in [2] and [5]. This section is useful to a practicing engineer to realize the advantages and disadvantages of different three-level PWM dc–dc converters before choosing a certain topology for their application. The modes of operation of the PWM three-level dc–dc converter with the proposed load adaptive ZVS auxiliary circuit are described in this section. Fig. 4 shows the current flow during each mode while Fig. 5 shows the ideal waveforms of the key components of the converter. The converter is controlled by the well-known phase-shift control method, which means that duty ratio of each switch is 0.5 with some dead time; the gating pulses of switches S2 and S3 are complimentary, while those of S1 and S4 are complimentary with a certain phase shift between the gating pulses of S2 and S3 , respectively. It is this phase shift that defines the duty ratio of the transformer primary voltage Vab and in turn, controls the output voltage. The clamping diodes D–c1 and D–c2 are provided to equalize the voltage across the semiconductor devices and to clamp the voltage Vab to zero whenever necessary.

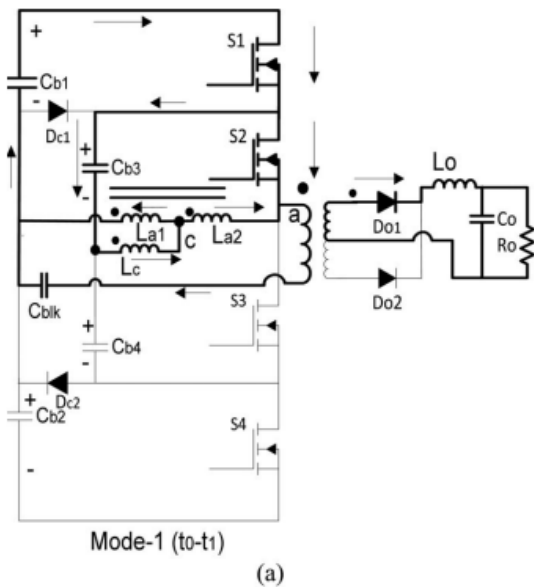
MODES OF OPERATION:

Mode 1 (t0 –t1):

An energy transfer mode. Switches S1 and S2 are conducting and energy is transferred from the upper dc bus capacitor Cb1 . The transformer primary voltage Vab is equal to VDC /2. Voltage Vac across La2 is +VDC /4 so that the net voltage across the coupled inductor LC during this mode is zero so the current in it remains constant. Also during this mode, a net positive voltage of (VDC /2–VoN) is incident across the combination of leakage inductance Llk and the reflected output inductor to the primary side so that the current in them starts increasing.

The key equation in this mode is

$$i_{lk}(t) = i_{lk}(t_0) + \frac{V_{Dc} - NV_0}{N^2 L_0 + L_{lk}}(t - t_0) \text{ for } (t_0 < t < t_1).$$



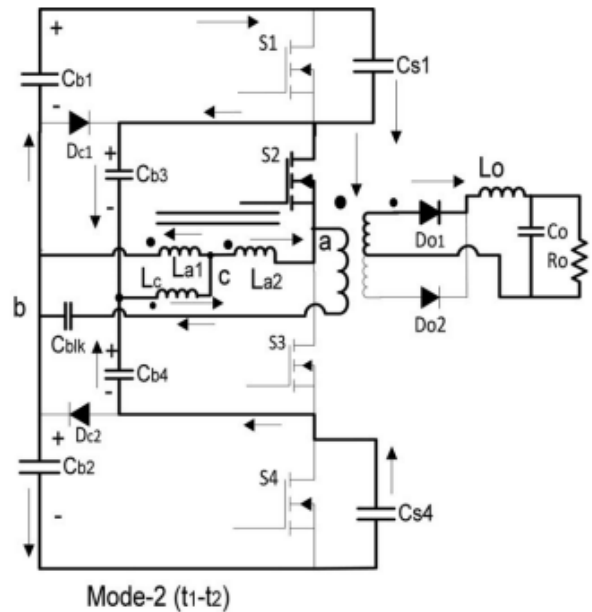
Mode 2 (t_1-t_2):

At time t_1 , which is also the duty ratio of the converter $DTSw/2$, switch S1 is turned OFF. The sum of currents in the auxiliary winding La2 and the current in the combined inductance of the leakage inductor and the reflected output inductor to the primary side charges and discharges the output capacitances of the switches S1 and S4, respectively. There is no change in the voltage or current waveform of the auxiliary inductors in this mode. Assuming that the values of the output inductor and the auxiliary inductor are large enough compared to the leakage inductor so that their currents can be considered to be constant during this mode, the key differential equations describing the switching transitions occurring in this mode are

$$C_{DS} \frac{dv_{S1}}{dt} = \frac{i_{aux}(t_1) + i_{Lo}(t_1)/N}{2}$$

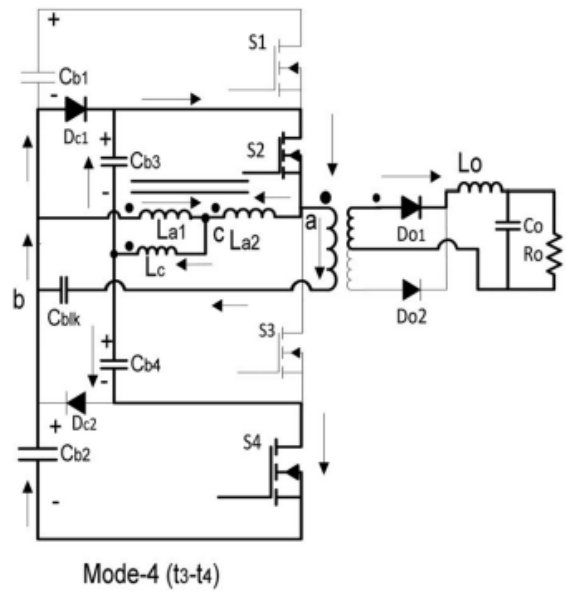
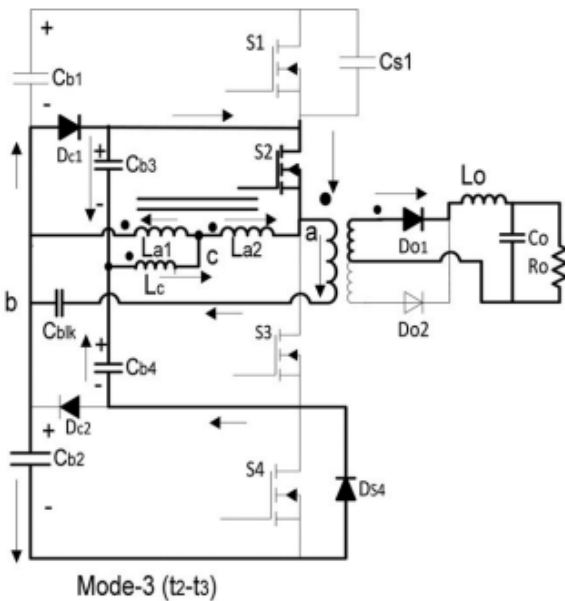
$$C_{DS} \frac{dv_{S4}}{dt} = \frac{V_{DC}}{2} - \frac{i_{aux}(t_1) + (i_{Lo}(t_1)/N)}{2}.$$

This mode ends with the voltage across S1 rising to $V_{DC}/2$. During modes 1 and 2, current in La1 is negative and current in La2 is positive.



Mode 3 (t_2-t_3):

This is a freewheeling mode with no energy being transferred to the output through the transformer, whose primary remains shorted in this mode. The clamping diode Dc1 starts to conduct and clamps the voltage of S1 at $V_{DC}/2$ while the voltage across S4 is zero. During this mode, there is a change in the voltage waveform of the coupled inductor La1 so that a net positive voltage of $+V_{DC}/4$ is incident across La1 and a negative voltage of $-V_{DC}/4$ reflected from La1 is incident across La2. In this mode, current in La1 begins to ramp up while that in La2 starts to ramp down; the output current flows through diode Do1. At the end of this mode, the inductor currents reverse their polarities at time t_3 .



Mode 4 (t_3-t_4):

At t_3 , the currents in the coupled inductor reverse their polarities and continue to slew at the same rate as given in mode 3. The current in switch S4 also reverses in this mode and flows through the bulk device. The transformer primary voltage V_{ab} still remains clamped to zero. Switch S2 is turned OFF at the end of this mode. It should be noted that the combined duration of modes 3 and 4 signify the zero state of the transformer primary voltage over half a switching cycle. The key equation for the transformer primary current during modes 3 and 4 is given by

$$\frac{d}{dt} i_{lk}(t - t_2) = -\frac{NV_o}{(L_{lk} + N^2 L_o)} \text{ for } (t_2 < t < t_4).$$

The duration of the combined modes 3 and 4 signify the zero state of the transformer primary voltage over half a switching cycle and is given by

$$(t_4 - t_2) \approx (1 - D) \frac{T_{Sw}}{2}.$$

Mode 5 (t_4-t_5):

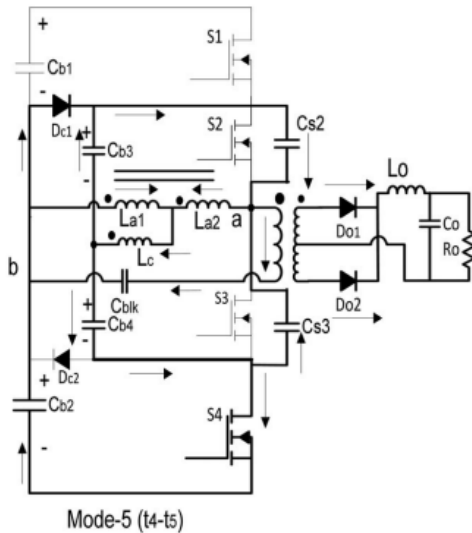
At t_4 , switch S2 is turned OFF. During this mode, the transformer leakage inductance is disconnected from the reflected output inductance and both output diodes Do1 and Do2 at the transformer secondary begin to conduct. The output inductor current freewheels through both output rectifiers and a negative voltage of $-V_o$ is incident across the output inductor. The current in the auxiliary inductor La2, along with the energy stored in the leakage inductor, charges and discharges the output capacitance of switches S2 and S3, respectively, to and from a voltage of $V_{DC} / 2$. At the end of this mode at t_5 , the output capacitors of S2 and S3 are charged to $V_{DC} / 2$ and discharged to zero, respectively, so that the body diode of S3 conducts. The transformer primary voltage also rises from zero to $V_{DC} / 2$ during this mode.

$$\frac{di_{Lk}}{dt} = -\frac{v_{Sw2}(t - t_4)}{L_{lk}} \text{ for } (t_4 < t < t_5)$$

$$\frac{dv_{Sw2}(t - t_4)}{dt} = \frac{1}{2C_{DS}} [i_{lk}(t - t_4) + i_{aux}(t_4)] \text{ for } (t_4 < t < t_5)$$

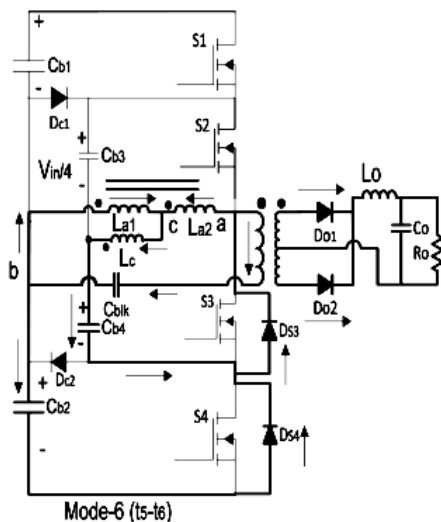
$$\frac{dv_{Sw3}(t - t_4)}{dt} = -\frac{1}{2C_{DS}} [i_{lk}(t - t_4) + i_{Aux}(t_4)] \text{ for } (t_4 < t < t_5)$$

At the end of this mode, clamping diode Dc1 stops conducting.



Mode 6 (t5 –t6) :

This mode is similar to mode 5 except that the body diode of S3 starts conducting so that S3 can be turned ON with ZVS. This mode ends with the transformer primary reducing to zero and undergoing phase reversal at time t6 . From this mode onward, till the turn-off of S4 , the transformer primary voltage remains clamped to $-V_{DC} /2$. During mode 6, current in S4 can flow either through the bulk device or through its body diode depending on the magnitude of the currents in the transformer primary and the currents in the coupled inductor.



Mode 7 (t6 –t7) :

At t6 , the transformer primary current starts reversing its phase and increases in a reverse direction until the magnitude of the current in the leakage inductor equals the current in the output inductor reflected at the transformer primary side at time t7 , during steady-state operation of the converter. At time t7 , another energy transfer mode begins and output diode Do2 conducts the transformer secondary current and S3 and S4 are conducting the transformer primary current. The equation describing the current in the leakage inductor during this mode is given by

$$i_{lk}(t - t_6) = -\frac{V_{DC}}{2L_{lk}}(t - t_6) \quad \text{for } (t_6 < t < t_7).$$

It should be noted that duration of this mode signifies lost duty ratio of the converter. So it is imperative to reduce the duration of this mode and the most effective way to do so is to reduce the leakage inductor.

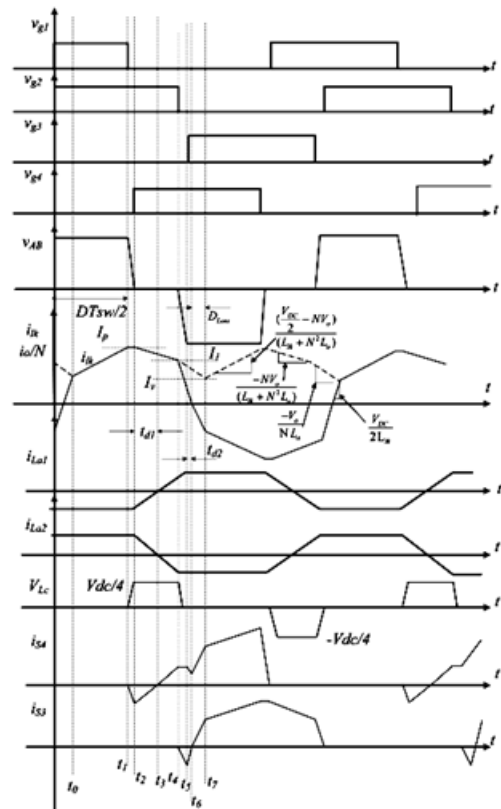


Fig. waveforms at steady-state operation.

The following can be concluded from the above discussion on the modes of operation:

1) It is this current given by (9), available from the couple inductor which is responsible for assisting ZVS of the bridge devices during modes 2 and 5. The current given by (10) is extremely significant in the sense that it signifies the peak ramp current magnitude in the coupled inductor and it is now a function of the duty ratio of the converter. The growth of ramp current in the auxiliary inductors depends on the duration of the nonenergy transfer modes or the freewheeling modes, i.e., modes 3 to 5 which is approximately $(1-D)T_{sw}/2$. The ramp current magnitude will be greater at lower loads when modes 3 to 5 are longer because of the smaller duty ratio of the converter, while the same ramp will have less opportunity to slew at higher loads when the duration of modes 3 to 5 are shorter. The assistance from the auxiliary circuit is most needed in terms of the ramp current during switching intervals at low loads when there is not enough energy in the leakage inductance to discharge switch capacitors, while the same assistance from the auxiliary circuit needs to be minimized as load increases since the energy in the leakage inductance increases as well leading to natural ZVS at higher loads. This feature is achieved by the proposed coupled inductor auxiliary circuit, which is simple, unique, and novel.

2) ZVS at no load is easily achieved since the ramp current magnitude is at its maximum at no load and can provide the sufficient amount of inductive current for discharging switch capacitances.

3) The component count of the converter is reduced and better component packaging can be achieved by having a coupled inductor auxiliary circuit instead of separate auxiliary inductors wound on separate cores.

ANALYSIS:

The analysis is based on an example specification as follows:

1) Input dc voltage: $V_{DC} = 800$ V;

2) Switching frequency: $f_{Sw} = 200$ kHz;

3) Output voltage: $V_o = 12$ V;

4) Output power P_o varies from 0 to 2.5 kW;

5) Transformer turns ratio : 24:1;

6) Output inductor : 1 μ H.

SOFTWARE TOOLS:

▶ Simulink

- It is a commercial tool for modeling, simulating and analyzing multi domain dynamic systems.
- Its primary interface is a graphical block diagramming tool and a customizable set of block libraries.
- Simulink is widely used in control theory and digital signal processing for multi domain simulation and Model based design.

▶ APPLICATIONS

1. Technical computing
2. Engineering and sciences applications
 - Electrical Engineering
 - DSP and DIP
 - Automation
 - Communication purpose
 - Aeronautical
 - Pharmaceutical
 - Financial services.

Other Features

- 2-D and 3-D graphics functions for visualizing data
- Tools for building custom graphical user interfaces
- Functions for integrating MATLAB based algorithms with external applications and languages, such as C, C++, Fortran, Java, COM, and Microsoft Excel.

ADVANTAGES:

- Strict efficiency requirements at loads from 20% to 50% of full load of ac–dc converters for telecom applications.
- Introduced by energy star enforcing industries to improve efficiency of the dc–dc converter in an ac–dc converter powering data-center loads at those loads.

APPLICATION:

- Advantage of this project is compared to the conventional dc–dc full-bridge converter in highvoltage applications is that the input dc voltage is split equally.
- So that the peak voltage stress of the semi-conductor devices and the dc bus capacitors are reduced to half of the input dc voltage.
- High-efficiency requirements at low and mid loads in high switching frequency PWM dc–dc three-level converters implemented with MOSFETs can be achieved
- By reducing switching losses through optimized load adaptive ZVS for the entire load range.

SIMULINK RESULTS AND OUTPUTS:

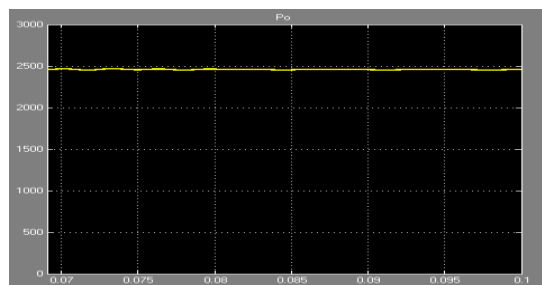
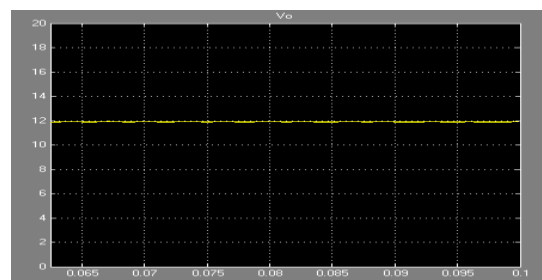
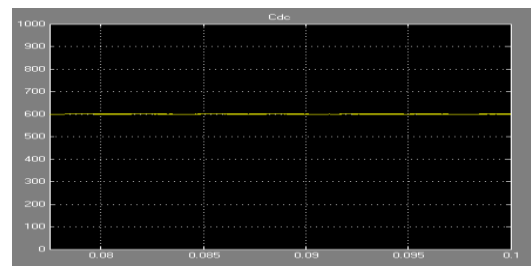
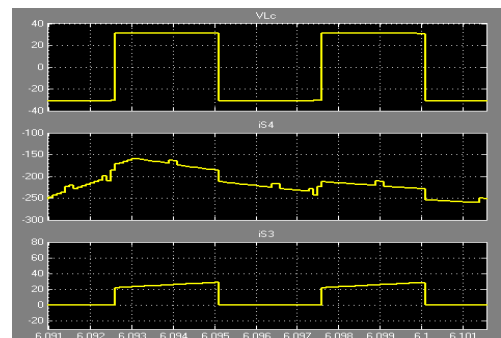
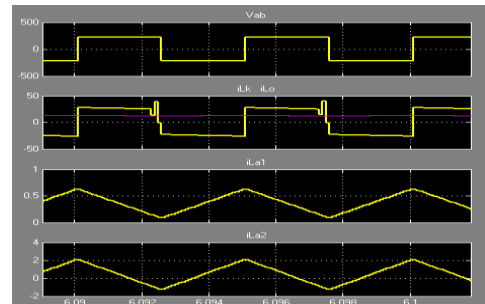
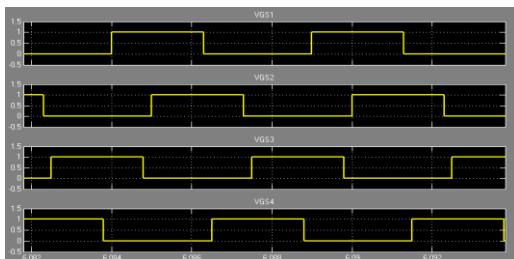
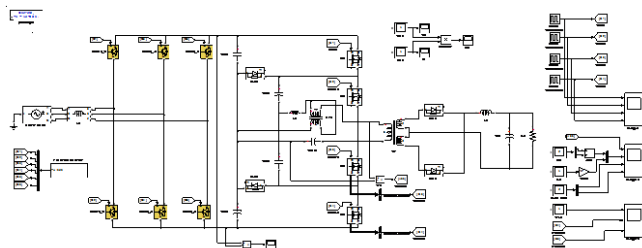


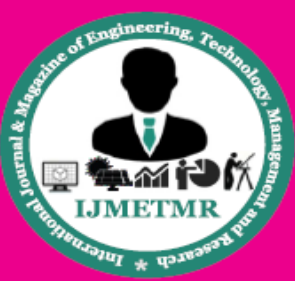
Fig:Output waveforms

VI. CONCLUSION:

Presently strict efficiency standards have been setup to reduce overall energy consumed by loads powered by the utility mains in data centers. In such applications, the power converters mostly operate between 20% of full load and 60% of full load, so higher efficiencies need to be achieved at these low and mid-range loads. To increase efficiency at such load range, load adaptive ZVS must be ensured for whole load range from no-load to full-load operation of the dc-dc converter of an ac-dc converter. In this paper, a novel yet simple auxiliary ZVS circuit for three-level dc-dc converters is proposed using a uniquely coupled inductor strategically placed in a PWM three-level dc-dc converter. The simple auxiliary circuit gives rise to a load adaptive ZVS. The operation of the proposed converter operation has been extensively discussed, analyzed, and validated by experimental results obtained from a laboratory prototype. The load adaptive approach helps the overall three-phase ac-dc converter which is a cascaded configuration of front-end three phase boost PWM converter and the proposed PWM three-level dc-dc isolated converter to conform to Energy Star Platinum Efficiency standard.

REFERENCES:

- [1] Y. Shi and X. Yang, "Wide range soft switching PWM three-level DC-DC converters suitable for industrial applications," *IEEE Trans. Power Electron.*, vol. 29, no. 2, pp. 603,616, Feb. 2014.
- [2] J. L. Duarte, J. Lokos, and F. B. M. van Horck, "Phase-shift-controlled three-level converter with reduced voltage stress featuring ZVS over the full operation range," *IEEE Trans. Power Electron.*, vol. 28, no. 5, pp. 2140-2150, May 2013.
- [3] J.R. Pinheiro and I. Barbi, "Three-level zero-voltage-switching PWMDCDC converters-a comparison," in *Proc. IEEE 26th Annu. Power Electron. Spec. Conf.*, 1995, pp. 914-919, vol. 2, no. 1.
- [4] W. Li, S. Zong, F. Liu, H. Yang, X. He, and B. Wu, "Secondary-side phase-shift-controlled ZVS DC/DC converter with wide voltage gain for high input voltage applications," *IEEE Trans. Power Electron.*, vol. 28, no. 11, pp. 5128-5139, Nov. 2013.
- [5] H. Ma, Y. Ji, and Y. Xu, "Design and analysis of single-stage power factor correction converter with a feedback winding," *IEEE Trans. Power Electron.*, vol. 25, no. 6, pp. 1460-1470, Jun. 2010.
- [6] S. Dusmez and A. Khaligh, "A charge-nonlinear-carrier-controlled reduced-part single-stage integrated power electronics interface for automotive applications," *IEEE Trans. Veh. Technol.*, vol. 63, no. 3, pp. 1091-1103, Mar. 2014.
- [7] R. Ramakumar and P. Chiradeja, "Distributed generation and renewable energy systems," in *Proc. 37th Intersoc. Energy Convers. Eng. Conf.*, 2002, pp. 716-724.
- [8] S. I. Mustapa, Y. P. Leong, and A. H. Hashim, "Issues and challenges of renewable energy development: A Malaysian experience," in *Proc. Int. Conf. Energy Sustainable Develop.: Issues Strategies*, 2010, pp. 1-6.
- [9] W. Kempton and S. Letendre, "Electric vehicles as a new power source for electric utilities," *Transp. Res. Part D, Transport Environ.*, vol. 2, pp. 157-175, 1997.
- [10] B. Kramer, S. Chakraborty, and B. Kroposki, "A review of plug-in vehicles and vehicle-to-grid capability," in *Proc. IEEE Ind. Electron.*, 2008, pp. 2278-2283.
- [11] U. K. Madawala, P. Schweizer, and V. V. Haerri, "'Living and mobility'— A novel multipurpose in-house grid interface with plug-in hybrid blue angel," in *Proc. IEEE Conf. Sustainable Energy Technol.*, 2008, pp. 531-536.
- [12] U. K. Madawala and D. J. Thrimawithana, "A bidirectional inductive power interface for electric vehicles in V2G systems," *IEEE Trans. Ind. Electron.*, vol. 58, no. 10, pp. 4789-4796, Oct. 2011.



[13] D. J. Thrimawithana, U. K. Madawala, R. Twiname, and D. M. Vilathgamuwa, "A novel matrix converter based resonant dual active bridge for V2G applications," in Proc. IPEC Conf. Power Energy, 2012, pp. 503–508.

[14] D. C. Erb, O. C. Onar, and A. Khaligh, "An integrated bi-directional power electronic converter with multi-level AC-DC/DC-AC converter and non-inverted buck-boost converter for PHEVs with minimal grid level disruptions," in Proc. IEEE Vehicle Power Propulsion Conf., 2010, pp. 1–6.